

1 GPU-based fast gamma index calculation

2 Xuejun Gu, Xun Jia, and Steve B. Jiang

3
4 Center for Advanced Radiotherapy Technologies and Department of Radiation
5 Oncology, University of California San Diego, La Jolla, CA 92037-0843

6
7 E-mail: sbjiang@ucsd.edu

8
9 The γ -index dose comparison tool has been widely used to compare dose
10 distributions in cancer radiotherapy. The accurate calculation of γ -index requires
11 an exhaustive search of the closest Euclidean distance in the high-resolution
12 dose-distance space. This is a computational intensive task when dealing with
13 3D dose distributions. In this work, we combine a geometric method (Ju et al.
14 *Med Phys* **35** 879-87, 2008) with a radial pre-sorting technique (Wendling et al.
15 *Med Phys* **34** 1647-54, 2007), and implement them on computer graphics
16 processing units (GPUs). The developed GPU-based γ -index computational tool
17 is evaluated on eight pairs of IMRT dose distributions. The GPU
18 implementation achieved 20x~30x speedup factor compared to CPU
19 implementation and γ -index calculations can be finished within a few seconds
20 for all 3D testing cases. We further investigated the effect of various factors on
21 both CPU and GPU computation time. The strategy of pre-sorting voxels based
22 on their dose difference values speed up the GPU calculation by about 2-4 times.
23 For n -dimensional dose distributions, γ -index calculation time on CPU is
24 proportional to the summation of γ^n over all voxels, while that on GPU is
25 effected by γ^n distributions and is approximately proportional to the γ^n
26 summation over all voxels. We found increasing dose distributions resolution
27 leads to quadratic increase of computation time on CPU, while less-than-
28 quadratic increase on GPU. The values of dose difference (DD) and distance-to-
29 agreement (DTA) criteria also have their impact on γ -index calculation time.

30
31 Submitted to *Physics in Medicine and Biology*

32 1. Introduction

33

34 The γ -index concept introduced by Low *et al.* (Low *et al.* 1998) has been widely used to
35 compare two dose distributions in cancer radiotherapy. The original γ -index calculation
36 algorithm of Low *et al.* (Low *et al.* 1998) has been improved for better accuracy and/or
37 efficiency (Depuydt *et al.* 2002; Bakai *et al.* 2003; Stock *et al.* 2005; Jiang *et al.* 2006;
38 Spezi and Lewis 2006). However, since these modified algorithms still involve
39 computational intensive tasks such as interpolation of dose grid and exhaustive search, it
40 is very time-consuming (*e.g.*, many minutes) to compare two 3D dose distributions of
41 clinically relevant sizes.

42 In more recent years, much effort has been invested to develop fast and/or accurate γ -
43 index calculation algorithms. Wendling *et al.* (Wendling *et al.* 2007) speeded up the
44 exhaustive search by pre-sorting involved evaluation dose points with respect to their
45 spatial distance to reference dose point and performing interpolation on-fly in a fixed
46 searching radius region. This fixed search region induces overestimation of γ -index
47 values at certain case if dose difference values are very large inside the search region and
48 has sharp drop just beyond the search region boundary. This algorithm also relies on fine
49 dose interpolation to secure accuracy. The geometric interpretation of γ -index evaluation
50 technique proposed by Ju *et al.* (Ju *et al.* 2008) implies a linear interpolation by
51 calculating the distance from a reference point to a subdivided simplex formed by
52 evaluation dose points in search regions. Thus, high accuracy and efficiency can be
53 achieved without interpolating dose grid to fine resolution. However, searching the
54 closest distance over all subdivided simplexes is still time-consuming. Later, Chen *et al.*
55 (Chen *et al.* 2009) reports a method based on using fast Euclidean distance transform
56 (EDT) of quantized n -dimensional dose distributions. Fast γ -index evaluation can be
57 achieved with complexity of $O(N^n M)$, where N is the size of dose distribution in each
58 dimension, n is the number of dimension, and M is the number of quantized values for
59 dose distribution. This method brings in discretization errors when quantizing dose
60 distributions. It also requires M time's more memory space of original searching based
61 algorithm. Thus, a full 3D application of EDT method is limited by its memory
62 requirement. The searching based algorithm's complexity is $O(N^n N_s)$, where N_s
63 represents exhaustive search steps. For cases where γ is not very large, where N_s is much
64 smaller than M , this EDT method loses its advantage of efficiency. Recently, Yuan *et al.*
65 (Yuan and Chen 2010) proposes a technique using a k -d tree technique for nearest
66 neighbor searching. The searching time for N^n voxels dose distribution can be reduced to
67 $(N^n)^{1/k}$, where $2 < k < 3$ for 2D and 3D dose distributions. However, this method
68 requires interpolating dose grid to secure accuracy. Moreover, in certain cases, the
69 overhead of k -d tree construction time is longer than γ -index calculation time.

70 Another approach to speed up γ -index evaluation is to implement an accurate
71 algorithm on graphics processing unit (GPU) platform. GPUs have recently been
72 introduced into the radiotherapy community to accelerate computational tasks including
73 CBCT reconstruction, deformable image registration, dose calculation, and treatment
74 plan optimization (Jia *et al.* 2010b; Samant *et al.* 2008; Sharp *et al.* 2007; Jacques *et al.*

2008; Hissoiny *et al.* 2009; Gu *et al.* 2010; Gu *et al.* 2009; Jia *et al.* 2010a; Men *et al.* 2009; Men *et al.* 2010a; Men *et al.* 2010b). GPU are especially well-suited for problems that can be expressed as data-parallel computations (NVIDIA 2010). γ -index calculation belongs to this category, because the evaluation of each reference point is totally independent. Instead of implementing the memory demanding EDT method or the large overhead k -d tree method, we decide to combine the accuracy of geometric interpretation technique (Ju *et al.* 2008) and the efficiency of the pre-sorting technique (Wendling *et al.* 2007). We will also revise this modified algorithm to make it GPU-friendly and then implement it on GPU to achieve both accuracy and high efficiency.

The remainder of this paper is organized as follows. In Section 2, we will discuss the modified γ -index algorithm and its implementation on GPU. Section 3 will present the evaluation of our GPU-based algorithm using eight 3D IMRT dose distributions pairs. We will first study the speedup factor achieved by GPU implementation. We will further study the effects of dose difference sorting and the r -index values on the computation time. We will also investigate how the dose distribution resolution and dose difference (DD) and distance-to-agreement (DTA) criteria impact on computation time. Conclusion will be given in Section 4.

92

93 2. Methods and Materials

94

95 2.1 A modified γ -index algorithm

96

97 The γ -index is the minimum Euclidean distance in normalized dose-distance space (Low
98 *et al.* 1998):

$$\gamma(\mathbf{r}_r) = \min\{\Gamma(\mathbf{r}_r, \mathbf{r}_e)\},$$

with

$$\begin{aligned} \Gamma(\mathbf{r}_r, \mathbf{r}_e) &= |\tilde{\mathbf{r}}_r - \tilde{\mathbf{r}}_e|, \forall \{\mathbf{r}_e\}, \\ \tilde{\mathbf{r}}_r &= \left(\frac{\mathbf{r}_r}{\Delta d}, \frac{D_r(\mathbf{r}_r)}{\Delta D} \right), \\ \tilde{\mathbf{r}}_e &= \left(\frac{\mathbf{r}_e}{\Delta d}, \frac{D_e(\mathbf{r}_e)}{\Delta D} \right). \end{aligned} \quad (1)$$

99

100 Here, $D_r(\mathbf{r}_r)$ is the reference dose distribution at position \mathbf{r}_r and $D_e(\mathbf{r}_e)$ is the evaluated
101 dose distribution at position \mathbf{r}_e . ΔD and Δd refer to dose DD criterion and DTA criterion,
102 respectively. Using geometric method (Ju *et al.* 2008), the accurate Γ can be obtained by
103 calculating the distance from the reference point $\tilde{\mathbf{r}}_r$ to the continuous evaluation surface
104 formed by discrete evaluation points $\tilde{\mathbf{r}}_e$. And the minimum Γ value is achieved by
105 accelerated exhaustive search with pre-sorting algorithm (Wendling *et al.* 2007). The
106 algorithm A1 illustrates the CPU implementation of combined presorting and geometric
107 γ -index algorithm.

108

109

110

111

112 **Algorithm A1:** A modified γ -index calculation algorithm implemented on CPU

113

- 114 1. Calculate the maximum DD: $\max(DD(\mathbf{r}_r)) = \max(D(\mathbf{r}_r) - D(\mathbf{r}_r))$, $\forall \{\mathbf{r}_r\}$;
 115 2. Calculate the geometric distance set L_n which defines the maximum search range
 116 for each reference point;

$$117 \quad L_n = \sqrt{(i\Delta x)^2 + (j\Delta y)^2 + (k\Delta z)^2} / \Delta d;$$

$$118 \quad \text{with } |i(\text{or } j, k)| \leq \frac{\max(DD(\mathbf{r}_r))}{\Delta D} \frac{\Delta d}{\Delta x(\text{or } \Delta y, \Delta z)} \ \& \ |L_n| < \frac{\max(DD(\mathbf{r}_r))}{\Delta D};$$

- 119 3. Sort the geometric distance set $\{n, L_n\}$ in ascending order of L_n ;
 120 4. For each reference dose point:
 121 a. Set $\gamma(\mathbf{r}_r) = DD(\mathbf{r}_r) / \Delta D$;
 122 b. For $n = 1: N$ (N is the length of $\{L_n\}$)
 123 i. Calculate Euclidean distance $\Gamma(\tilde{\mathbf{r}}_r, S_n)$ from reference point $\tilde{\mathbf{r}}_r$ to a k -
 124 simplex S_n : $\Gamma(\tilde{\mathbf{r}}_r, S_n) = \min |\tilde{\mathbf{r}}_r - \sum_{i=1}^{k+1} \omega_i v_i|$;
 125 ii. If $\Gamma(\tilde{\mathbf{r}}_r, S_n) > L_n$: break;
 126 iii. If $\Gamma(\tilde{\mathbf{r}}_r, S_n) < \gamma(\mathbf{r}_r)$: $\gamma(\mathbf{r}_r) = \Gamma(\tilde{\mathbf{r}}_r, S_n)$;
 127 END

128

129 Similar to Wendling *et al.* (Wendling *et al.* 2007), at the Steps 2 and 3 of Algorithm
 130 A1, we establish a sorted table of normalized geometric distance $\{L_n\}$ of all the voxels in
 131 the maximum search range. However, instead of using a manually selected search range
 132 as in (Wendling *et al.* 2007), we choose search radius $\max(DD(\mathbf{r}_r)) \Delta d / \Delta D$, which can
 133 avoid overestimating γ -index value.

134 The $\Gamma(\tilde{\mathbf{r}}_r, S_n)$ in Algorithm A1 Step 4 is obtained when $\{\omega_1, \dots, \omega_k\} =$
 135 $(V^T V)^{-1} V^T P$, $\omega_{k+1} = 1 - \sum_{i=1}^k \omega_i$, where P and V are $K \times 1$ and $K \times k$ matrices with a

$$136 \quad \text{form } P = \begin{Bmatrix} c_1(\tilde{\mathbf{r}}_r) - c_1(v_{k+1}) \\ \vdots \\ c_n(\tilde{\mathbf{r}}_r) - c_n(v_{k+1}) \end{Bmatrix}, V = \begin{Bmatrix} c_1(v_1) - c_1(v_{k+1}) & \cdots & c_1(v_k) - c_1(v_{k+1}) \\ \vdots & & \vdots \\ c_n(v_1) - c_n(v_{k+1}) & \cdots & c_n(v_k) - c_n(v_{k+1}) \end{Bmatrix}.$$

137 Here, for a k -dimensional dose distribution $K = k + 1$, $c_j(q)$ is the j th coordinate of point
 138 of q . Regarding $\Gamma(\tilde{\mathbf{r}}_r, S_n)$ calculation, we follow the computational acceleration
 139 techniques presented by Ju *et al.* (Ju *et al.* 2008), where the computation is conducted
 140 recursively in the simplex set and the recursive computation is only limited to the
 141 subset of simplex where corresponding weights ω_i are negative. Detailed information
 142 regarding $\Gamma(\tilde{\mathbf{r}}_r, S_n)$ calculation can be found in the reference (Ju *et al.* 2008).

143

144 2.2 GPU implementation

145

146 In this work, we implement the γ -index algorithm (Algorithm A1) on GPU using
 147 Compute Unified Device Architecture (CUDA) programming environment. In the
 148 Algorithm A1 Step 4, for each reference point the minimum Γ value is searched around
 149 the reference point in a search range of a radius $(DD(\mathbf{r}_r) / \Delta D) \Delta d$. On CPU, Step 4 is
 150 repeated for all reference points in a sequential manner. On GPU, this step can be

151 parallelized for a large number of reference points and executed simultaneously using
 152 multiple threads. A key point of the GPU implementation of this algorithm is to ensure all
 153 threads in the same batch (strictly speaking *warp* in CUDA terminology) to have similar
 154 numbers of arithmetic operations. This is because, if some threads in a warp require much
 155 longer execution time, the other threads in this warp will finish first and then wait in idle
 156 until the longer execution time threads finish, implying a waste of computational power.
 157 Therefore, directly mapping the CPU version γ -index algorithm (Algorithm A1) onto
 158 GPU cannot guarantee that all threads in a warp have similar computation burden, and
 159 consequentially cannot achieve maximum speed up. As we know, the upper boundary of
 160 the search range for each reference point is $(DD(\mathbf{r}_r)/\Delta D)\Delta d$. The computation task for
 161 each reference point is then approximately proportional to the dose difference $DD(\mathbf{r}_r)$.
 162 The larger the $DD(\mathbf{r}_r)$, the more evaluation dose points will be involved, leading to
 163 longer computation time. We therefore pre-sort the voxels according to $DD(\mathbf{r}_r)$ (for
 164 convenience we call it DD sorting) and perform γ -index calculation on GPU according to
 165 pre-sorted voxel order. This DD-sorting procedure, along with pre-sorting the geometric
 166 distance set $\{n, L_n\}$, can be parallelized using recently developed Thrust library
 167 functions (Hoberock *et al.* 2010), which can sort a (or multiple) millions-element array(s)
 168 within subseconds. The completed GPU-based γ -index algorithm is illustrated as
 169 following:

170

171 **Algorithm A2:** A modified γ -index calculation algorithm implemented on GPU

172

-
- 173 1. Transfer dose distributions data from CPU to GPU;
 - 174 2. CUDA Kernel 1: calculate in parallel the dose difference
 175 $DD(\mathbf{r}_r) = D(\mathbf{r}_r) - D(\mathbf{r}_r), \forall \{\mathbf{r}_r\};$
 - 176 3. Sort in parallel $\{\text{Voxel Index}, DD(\mathbf{r}_r)\}$ array pair in ascending order of $DD(\mathbf{r}_r)$
 177 using Thrust parallel sorting function and obtain $\max(DD(\mathbf{r}_r))$;
 - 178 4. CUDA Kernel 2: calculate in parallel the geometric distance set $\{L_n\}$;
 - 179 5. Sort in parallel the geometric distance set $\{n, L_n\}$ in ascending order of L_n
 180 using Thrust parallel sorting function;
 - 181 6. CUDA Kernel 3: calculate in parallel the γ -index values using the algorithm
 182 illustrated in Step 4 of Algorithm A1 ;
 - 183 7. Sort $\{\text{Voxel Index}, \gamma\}$ back to the original voxel index order;
 - 184 8. Transfer the γ -index data from GPU to CPU.
-

185

186 We would like to point out that the Step 4-b-i of Algorithm A1 utilizes a recursive
 187 algorithm for computing $\Gamma(\tilde{\mathbf{r}}_r, S_n)$ only in the subset of simplexes which involves many
 188 IF conditions and thus creates a branching issue in GPU implementation. To avoid this
 189 problem, in Step 6 (Kernel 3) of Algorithm A2, we calculate $\Gamma(\tilde{\mathbf{r}}_r, S_n)$ in all simplexes.

190

191

192

193

194 3. Experimental Results and Discussion

195

196 3.1 Experimental data sets

197

198 We tested our GPU implementation on eight IMRT dose-distribution pairs (4 lung cases
 199 (L1-L4) and 4 head-neck cases (H1-H4)), which were generated using a Monte Carlo
 200 dose engine called MCSIM (Ma *et al.* 2002) as well as an in-house developed pencil
 201 beam algorithm (Gu *et al.* 2009). Monte Carlo dose calculation results were treated as the
 202 reference dose distributions while results obtained from the pencil beam algorithm were
 203 used as the evaluation dose distributions. All the doses were originally calculated with the
 204 voxel size of $4.0\text{mm} \times 4.0\text{mm} \times 2.5\text{mm}$ and normalized to the prescription dose and
 205 interpolated to various resolution levels for comparison studies. CPU computation was
 206 conducted on a 4-core Intel Xeon 2.27 GHz processor. GPU computation was performed
 207 on one single NVIDIA Tesla C1060 card. We would like to point out that our GPU
 208 implementation did not affect the calculation accuracy; in all scenarios, the γ -index
 209 values calculated on GPU agree with those calculated on CPU within $\sim 10^{-6}$. In the
 210 following sections, we present results under various conditions. For the CPU
 211 implementation based on Algorithm A1, we divide the total computation time T^C into
 212 two parts, *i.e.*, $T^C = T_p^C + T_\gamma^C$, where T_p^C is the data processing time (Steps 1, 2, and 3 of
 213 Algorithm A1) and T_γ^C is the γ -index calculation time (Step 4 of Algorithm A1). For the
 214 GPU implementation based on Algorithm A2, we split the total computation time T^G into
 215 three parts, *i.e.*, $T^G = T_t^G + T_p^G + T_\gamma^G$, where T_t^G is the data transferring time between
 216 CPU and GPU (Steps 1 and 8 of Algorithm A2), T_p^G is the data processing time (Steps 2-
 217 5 and Step 7 of Algorithm A2), and T_γ^G is the γ -index calculation time (Step 6 of
 218 Algorithm A2).

219

220 3.2 Speedup of GPU vs. CPU

221

222 For this study, we set the resolution of dose distributions to be $256 \times 256 \times$
 223 144 (or $160, 206$) and use 3% for DD criterion and 3 mm for DTA criterion. Table 1
 224 lists computation time for the CPU implementation (Algorithm A1) and the GPU
 225 implementation (Algorithm A2). We present two speedup factors in Table 1, with and
 226 without CPU-GPU data transferring time, *i.e.*, T^C/T^G and $T^C/(T^G - T_t^G)$. These two
 227 speedup factors are quite similar (within 3% for all cases), indicating that the data
 228 transferring time in GPU calculation is not significant compared to γ -index computation
 229 time T_γ^G . We can also see that the data processing time in both CPU and GPU
 230 implementations is relatively insignificant compared to the γ -index calculation time (Step
 231 4 of Algorithm A1 and Step 6 of Algorithm A2). Overall, the GPU implementation can
 232 achieve about 20x~30x speedup compared to its CPU implementation.

233

234

235

Table 1: Calculation time of γ -index for CPU and GPU implementations for 8 IMRT dose distribution pairs.

Case	Voxel number	CPU (sec)			GPU (sec)				Speedup factor	
		T_p^C	T_γ^C	T^C	T_t^G	T_p^G	T_γ^G	T^G	$T^C/(T^G - T_t^G)$	T^C/T^G
L1	256×256×206	0.33	64.93	65.26	0.07	0.18	2.78	3.03	22.05	21.54
L2	256×256×160	0.24	65.64	65.89	0.06	0.15	2.40	2.61	25.84	25.25
L3	256×256×160	0.28	101.46	101.74	0.06	0.14	3.77	3.97	26.02	25.53
L4	256×256×160	0.25	30.10	30.35	0.06	0.14	0.86	1.06	30.35	28.63
H1	256×256×144	0.49	47.73	47.95	0.05	0.11	2.28	2.44	20.06	19.65
H2	256×256×144	0.45	242.23	242.68	0.05	0.12	7.56	7.73	31.60	31.39
H3	256×256×144	0.24	116.14	116.38	0.05	0.12	4.76	4.93	23.85	23.61
H4	256×256×144	0.22	107.61	107.86	0.05	0.12	4.21	4.38	24.91	24.63

236

237

3.3 The effect of DD sorting on computation time T_γ^G

238

239

240

241

242

243

As mentioned in Section 2.2, introducing of DD sorting (Step 3 in Algorithm A2) can better synchronize the computational tasks on CUDA threads and consequently to reduce the computation time. We illustrate the effect of DD sorting on T_γ^G in Table 2. The speedup achieved by DD sorting is around 2.3-4.9 times.

Table 2: Speedup achieved in GPU computation by sorting voxels based on the dose difference values.

Case	T_γ^G (Non-DD sorting) (sec)	T_γ^G (DD sorting) (sec)	Speedup factor achieved by DD sorting
L1	7.37	2.78	2.65
L2	7.47	2.40	3.11
L3	11.00	3.77	2.91
L4	1.99	0.86	2.31
H1	8.48	2.28	3.72
H2	24.50	7.56	3.24
H3	15.00	4.76	3.15
H4	20.6	4.21	4.90

244

245

3.4 The effect of γ -index value on computation time T_γ^C and T_γ^G

246

247

248

249

250

251

252

253

254

From Table 1, we see that, both T_γ^C and T_γ^G change significantly from case to case. Take cases L3 and L4 as an example, they have the same number of voxels, but their γ -index calculation time differs by more than 3 times. We know that computation time t for each reference point is proportional to the number of voxels searched N_s , *i.e.*, $t \propto N_s$. The relationship of N_s with the search length L can be expressed as $N_s \propto L^n$, where n is the dimension of dose distributions. Here, for all the testing cases in this paper, $n = 3$. On the other hand, from Algorithm A1 Step 4-b-ii, we can deduce the search length L is proportional to the γ value at each reference point, *i.e.*, $L \propto \gamma$. Thus, we can state that the

255 computation time t for each reference point is proportional to γ^n : $t \propto \gamma^n$. In Figure 1(a),
 256 we plot T_γ^C and T_γ^G versus the summation of γ^3 over all voxels ($\sum \gamma^3$) for each of 8
 257 testing cases, respectively. We see that both T_γ^C and T_γ^G are monotonically increasing with
 258 the value of $\sum \gamma^3$. To further illustrate our point, we choose one set of patient data (H2)
 259 and shift the evaluation dose distribution (normalized to the prescription dose) by -10%,
 260 -9%, ..., up to 10%, at a step size of 1%, inside the region of 10% iso-dose line. Figure
 261 1(b) illustrates the γ -index calculation time T_γ^C and T_γ^G with respect to $\sum \gamma^3$. We can see
 262 that T_γ^C versus $\sum \gamma^3$ can be fitted with a straight line (dashed line in Figure 1(b)),
 263 indicating that T_γ^C strictly follows the rule $T_\gamma^C \propto \sum \gamma^3$. However, the data points for T_γ^G
 264 are much more scattered. This is because the GPU computation time is not only the
 265 function of $\sum \gamma^3$, but also the function of γ^n distribution that determines the variation of
 266 threads computation time in a warp.
 267

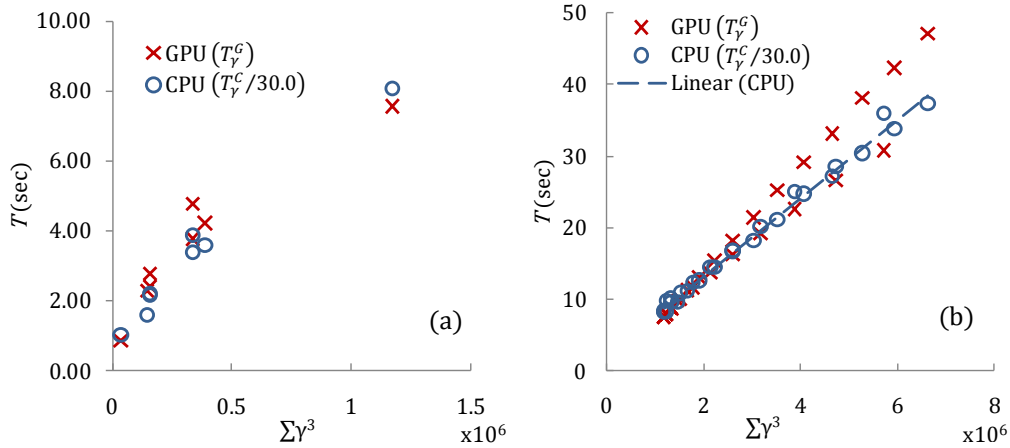


Figure 1: (a) GPU and CPU computation time for eight testing cases vs. the summed γ^3 value. (b) GPU and CPU computation time for case H2 with various dose shifts on evaluation dose distribution vs. the summed γ^3 value. For convenient purpose, we scaled down CPU computation time by a factor of 30.0 to illustrate them in the same vertical axis of GPU computation time.

268

269 3.5 The effect of dose distribution resolution on the computation time T_γ^C and T_γ^G

270

271 We choose the case H2 to test the effect of the dose distribution resolution on
 272 computation time T_γ^C and T_γ^G . We interpolate the dose distributions to various resolution
 273 levels, including $128 \times 128 \times 144$, $256 \times 256 \times 72$, $256 \times 256 \times 144$, and $512 \times$
 274 512×72 . We illustrate T_γ^C and T_γ^G changes with respect to the resolution changes in
 275 Figure 2. As indicated by the power trend lines (dashed lines in Figure 2), T_γ^C increases
 276 approximately as $N^{1.90}$ while T_γ^G increases approximately as $N^{1.68}$, when the resolution
 277 of dose distribution increases N times. As illustrated in Algorithm A1, the CPU based γ -
 278 index calculation is completed with two loops. The outer loop is over all the reference
 279 dose points and the inner loop is the exhaustive search in a limited region around each
 280 reference dose point. The computation time of the outer loop is increased linearly with

281 respect to the increase of resolution of dose distributions. The inner loop computation
 282 time is proportional to the number of voxels involved. For the geometric method, the
 283 number of involved voxels in a fixed region is increased linearly as the resolution
 284 increases. Overall, it leads to a quadratic increase of computational time ($\propto N^{1.90}$) for a
 285 linear change of resolution. For the GPU algorithm A2, the computation time increases as
 286 $(N)^{1.68}$ in this testing case. This slight difference might be due to the fact that the
 287 memory accessing time can be hidden by large arithmetic operations in GPU
 288 computation.
 289

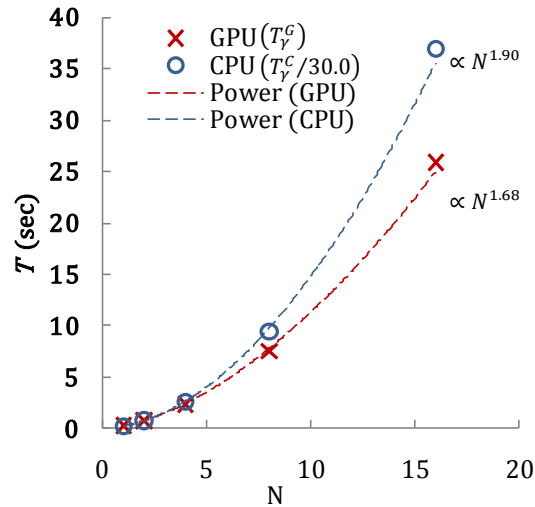


Figure 2. CPU and GPU computation time as functions of dose distribution resolution. Again, For convenient purpose, we scaled down CPU computation time by a factor of 30.0 to illustrate CPU computation time in the same axis of GPU computation time.

290

291 3.6 The effect of DD and DTA criteria on computation time T_γ^C and T_γ^G

292

293 In this study, we choose case H2 and fix the resolution to $256 \times 256 \times 144$, then vary
 294 DD and DTA criteria. Table 3 lists the computation time obtained from varying criteria.
 295 There are three interesting phenomena: 1) when we increase DD criterion value and fix
 296 the DTA criterion value, the computation time decreases; 2) when we fix DD criterion
 297 value and increase DTA criterion value, the computation time decrease; 3) when we
 298 increase both DD criterion value and DTA criterion value proportionally, for example,
 299 from 1%, 1mm to 2%, 2mm, or 3%, 3mm, the computation time does not change. As we
 300 mentioned in Section 3.4, the γ -index calculation time for each reference dose point $t \propto$
 301 γ^n . For phenomenon 1), when we increase DD criterion value and fix DTA criterion
 302 value, the γ -index value decreases. Consequently, the required searching steps decreases,
 303 and computation time decreases. For phenomenon 2), when we fixe DD criterion value,
 304 but increase DTA criterion value by k times, the γ -index values will decrease by k'
 305 times, with $k' < k$, which decreases computation time by $(k')^n$ times. However, when
 306 DTA criterion value increases by k times, the resolution in the normalized dose-distance
 307 space will also increase by k^n times, which consequently increases the computation time

308 by k^n times. The net change of the computation time should be $(k/k')^n$. Since $k' < k$,
 309 the overall computation time will then increase. For phenomenon 3), when we increase
 310 both DTA and DD criteria values simultaneously by k times, the γ -index values decrease
 311 by $k' = k$ times. The increase rate of computation time will be $(k/k)^n = 1$. The
 312 computation time under this situation will not change. From Table 3, we can see that the
 313 change of DD and DTA criteria values does not affect the speedup factor achieved with
 314 GPU implementation.
 315

Table 3: CPU and GPU computation time varies with DD and DTA criteria values.

DD criteria	DTA criteria (mm)	Computational time (sec)		Speedup factor T_Y^C/T_Y^G
		T_Y^G	T_Y^C	
1%	1	7.56	240.37	31.79
1%	2	26.31	863.33	32.81
1%	3	52.96	1545.09	29.17
2%	1	2.27	74.27	32.72
2%	2	7.56	265.82	35.16
2%	3	15.62	486.68	31.16
3%	1	1.27	40.09	31.57
3%	2	3.70	119.32	32.25
3%	3	7.56	245.34	32.45

316

317 4. Conclusions

318

319 In this paper, we implemented a modified γ -index algorithm on GPU. We evaluated our
 320 GPU implementation on eight pairs of IMRT dose distributions. Overall, our GPU
 321 implementation has achieved about 20x~30x speedup compared to the CPU
 322 implementation and can finish the γ -index calculation within a few seconds. We also
 323 studied the effects of various factors on the calculation time on both CPU and GPU. We
 324 found that the pre-sorting procedure based on the dose difference speeds up the GPU
 325 calculation by about 2~4 times. The CPU computation time is proportional to the
 326 summation of γ^n over all voxels, where n is the dimension of dose distributions. The
 327 GPU computation time is approximately proportional to the summation of γ^n over all
 328 voxels, but affected by the variation of γ^n among different voxels. We also found that
 329 increasing the resolution of dose distribution leads to a quadratic increase of computation
 330 time on CPU, while less-than-quadratic increase on GPU. We observed that both CPU
 331 and GPU computation time decrease when increasing DD criterion value and fixing DTA
 332 criterion value, increase when increasing DTA criterion value and fixing DD criterion
 333 value, and don't vary when DD criterion value and DTA criterion value both change
 334 proportionally. Both CPU and GPU codes developed in this work for γ -index dose
 335 evaluation are in public domain and available upon request.

336

337

338

339

Acknowledgements

341

342 This work is supported in part by the University of California Lab Fees Research
343 Program and by an NIH/NCI grant 1F32 CA154045-01. We would like to thank NVIDIA
344 for providing GPU cards for this project.

345

346

347 **Reference**

348

- 349 Bakai A, Alber M and Nusslin F 2003 A revision of the gamma-evaluation concept for
350 the comparison of dose distributions *Phys. Med. Biol.* **48** 3543-53
- 351 Chen M L, Lu W G, Chen Q, Ruchala K and Olivera G 2009 Efficient gamma index
352 calculation using fast Euclidean distance transform *Phys. Med. Biol.* **54** 2037-47
- 353 Depuydt T, Van Esch A and Huyskens D P 2002 A quantitative evaluation of IMRT dose
354 distributions: refinement and clinical assessment of the gamma evaluation
355 *Radiotherapy and Oncology* **62** 309-19
- 356 Gu X J, Choi D J, Men C H, Pan H, Majumdar A and Jiang S B 2009 GPU-based ultra-
357 fast dose calculation using a finite size pencil beam model *Phys. Med. Biol.* **54**
358 6287-97
- 359 Gu X J, Pan H, Liang Y, Castillo R, Yang D S, Choi D J, Castillo E, Majumdar A,
360 Guerrero T and Jiang S B 2010 Implementation and evaluation of various
361 demons deformable image registration algorithms on a GPU *Phys. Med. Biol.* **55**
362 207-19
- 363 Hissoiny S, Ozell B and Despres P 2009 Fast convolution-superposition dose calculation
364 on graphics hardware *Medical Physics* **36** 1998-2005
- 365 Hoberock J, Bell N and 2010 Thrust: A Parallel Template Library
- 366 Jacques R, Taylor R, Wong J and McNutt T 2008 Towards Real-Time Radiation
367 Therapy: GPU Accelerated Superposition/Convolution. In: *High-*
368 *Performance MICCAI Workshop*,
- 369 Jia X, Gu X J, Sempau J, Choi D, Majumdar A and Jiang S B 2010a Development of a
370 GPU-based Monte Carlo dose calculation code for coupled electron-photon
371 transport *Phys. Med. Biol.* **55** 3077-86
- 372 Jia X, Lou Y F, Li R J, Song W Y and Jiang S B 2010b GPU-based fast cone beam CT
373 reconstruction from undersampled and noisy projection data via total variation
374 *Medical Physics* **37** 1757-60
- 375 Jiang S B, Sharp G C, Neicu T, Berbeco R I, Flampouri S and Bortfeld T 2006 On dose
376 distribution comparison *Phys. Med. Biol.* **51** 759-76
- 377 Ju T, Simpson T, Deasy J O and Low D A 2008 Geometric interpretation of the gamma
378 dose distribution comparison technique: Interpolation-free calculation *Medical*
379 *Physics* **35** 879-87
- 380 Low D A, Harms W B, Mutic S and Purdy J A 1998 A technique for the quantitative
381 evaluation of dose distributions *Medical Physics* **25** 656-61
- 382 Ma C-M, Li J S, Pawlicki T, Jiang S B, Deng J, Lee M C, Koumrian T, Luxton M and
383 Brain S 2002 A Monte Carlo dose calculation tool for radiotherapy treatment
384 planning *Phys. Med. Biol.* **47** 1671
- 385 Men C H, Gu X J, Choi D J, Majumdar A, Zheng Z Y, Mueller K and Jiang S B 2009
386 GPU-based ultrafast IMRT plan optimization *Phys. Med. Biol.* **54** 6565-73
- 387 Men C H, Jia X and Jiang S B 2010a GPU-based ultra-fast direct aperture optimization
388 for online adaptive radiation therapy *Phys. Med. Biol.* **55** 4309-19
- 389 Men C H, Jia X, Jiang S B and Romeijn H E 2010b Ultrafast treatment plan optimization
390 for volumetric modulated arc therapy (VMAT) *Medical Physics* **37** 5787-91
- 391 NVIDIA 2010 NVIDIA CUDA Compute Unified Device Architecture, Programming
392 Guide version 3.2. ed NVIDIA
- 393 Samant S S, Xia J Y, Muyan-Ozcelilk P and Owens J D 2008 High performance
394 computing for deformable image registration: Towards a new paradigm in
395 adaptive radiotherapy *Medical Physics* **35** 3546-53

- 396 Sharp G C, Kandasamy N, Singh H and Folkert M 2007 GPU-based streaming
397 architectures for fast cone-beam CT image reconstruction and demons
398 deformable registration *Phys. Med. Biol.* **52** 5771-83
- 399 Spezi E and Lewis D G 2006 Gamma histograms for radiotherapy plan evaluation
400 *Radiotherapy and Oncology* **79** 224-30
- 401 Stock M, Kroupa B and Georg D 2005 Interpretation and evaluation of the gamma index
402 and the gamma index angle for the verification of IMRT hybrid plans *Phys. Med.*
403 *Biol.* **50** 399-411
- 404 Wendling M, Zijp L J, McDermott L N, Smit E J, Sonke J J, Mijnheer B J and Van Herk
405 M 2007 A fast algorithm for gamma evaluation in 3D *Medical Physics* **34** 1647-
406 54
- 407 Yuan J K and Chen W M 2010 A gamma dose distribution evaluation technique using the
408 k-d tree for nearest neighbor searching *Medical Physics* **37** 4868-73
409